Mechanical Domain Parametric Amplification

Jeffrey F. Rhoads
School of Mechanical Engineering,
Purdue University,
West Lafayette, IN 47907
e-mail: jfrhoads@purdue.edu

Nicholas J. Miller
e-mail: mille820@msu.edu

Steven W. Shaw
e-mail: shawsw@egr.msu.edu

Brian F. Feeny
e-mail: feeny@egr.msu.edu

Department of Mechanical Engineering,
Michigan State University,
East Lansing, MI 48824

Though utilized for more than 50 years in a variety of power and communication systems, parametric amplification, the process of amplifying a harmonic signal with a parametric pump, has received very little attention in the mechanical engineering community. In fact, only within the past 15–20 years has the technique been implemented in micromechanical systems as a means of amplifying the output of resonant microtransducers. While the vast potential of parametric amplification has been demonstrated, to date, in a number of micro- and nanomechanical systems (as well as a number electrical systems), few, if any, macroscale mechanical amplifiers have been reported. Given that these amplifiers are easily realizable using larger-scale mechanical systems, the present work seeks to address this void by examining a simple representative example: a cantilevered beam with longitudinal and transverse base excitations. The work begins with the systematic formulation of a representative system model, which is used to derive a number of pertinent metrics. A series of experimental results, which validate the work's analytical findings, are subsequently examined, and the work concludes with a brief look at some plausible applications of parametric amplification in macroscale mechanical systems.
[DOI: 10.1115/1.2980382]

1 Introduction

Parametric amplification, the process of amplifying an external harmonic signal with a parametric pump, is a well established concept in the field of electrical engineering, where it has been employed for more than 50 years in applications ranging from power and communication systems to Josephson junctions [1,2]. Though the technique has been widely implemented in electrical systems, parametric amplification has received comparatively little attention in mechanical engineering circles. In fact, only within the past 15–20 years has the technique been implemented in micromechanical systems as a means of amplifying, with minimal noise, the output of resonant microtransducers. The classical investigation of mechanical domain parametric amplification, completed by Rugar and Grütter in 1991, considered low-noise resonant amplification and noise squeezing in a microcantilever actuated by both piezoelectric and electrostatic elements [3]. Subsequent studies have built upon this seminal work by examining the feasibility of both degenerate (where the pump is locked at twice the frequency of the external signal) and nondegenerate (where the pump is locked at a frequency distinct from twice that of the external signal) manifestations of parametric low-noise signal amplification in a variety of resonant microsystems, including torsional microresonators [4,5], electric force microscopes [6], optically excited micromechanical oscillators [7], microring gyroscopes [8], microelectromechanical system (MEMS) diaphragms [9], coupled microresonators [10], and microcantilevers [11–13].

While the literature detailed above has demonstrated the vast potential of parametric amplification at the micro- and nanoscales, few, if any, macroscale mechanical amplifiers have been reported. Given that these amplifiers are easily realizable at larger scales, the present work seeks to address this void by examining a simple macroscale parametric amplifier. Specifically, the work details a joint analytical and experimental investigation of mechanical domain parametric amplification in a cantilevered beam with longitudinal and transverse base excitations. This paper begins in the following section with the development of a consistent lumped-mass model for the macroscale amplifier that is amenable to analysis. Following this, analytical results, obtained using the method of averaging, are detailed. The results acquired during the course of experimentation are presented in the subsequent section, and the work concludes with a brief discussion of the potential macroscale applications of parametric amplification.

Contributed by the Technical Committee on Vibration and Sound of ASME for publication in the JOURNAL OF VIBRATION AND ACOUSTICS. Manuscript received August 21, 2007; final manuscript received May 16, 2008; published online October 15, 2008. Assoc. Editor: I. Y. (Steve) Shen. Paper presented at the ASME 2007 Design Engineering Technical Conferences and Computers and Information in Engineering Conference (DETC2007), Las Vegas, NV, September 4–7, 2007.

2 Modeling

Though parametric amplification can be easily realized in a large number of macroscale systems, the present work, as noted above, limits itself to a simple representative example: a base-excited cantilever, such as that depicted schematically in Fig. 1. Given that the equation of motion governing the transverse dynamics of this system can be recovered using the energy-based methods previously presented in Refs. [14,15], only an outline of the procedure is detailed here.

Assuming that the cantilever beam is uniform and has negligible rotational inertia, the specific Lagrangian associated with the system can be approximated by

$$\bar{L} = \tfrac{1}{2}\rho A[(\dot{u}+\dot{u}_p)^2 + (\dot{v}+\dot{v}_p)^2] - \tfrac{1}{2}EI(\psi')^2 \tag{1}$$

where u, v, and ψ are defined as in Fig. 1, $(\dot{\bullet})$ and $(\bullet)'$ represent the temporal and spatial derivatives (determined with respect to time t and arc length variable s), u_p and v_p specify the imposed base motion in the longitudinal and transverse directions, and ρ, A, E, and I represent the beam's mass density, cross-sectional area, modulus of elasticity, and cross-sectional moment of inertia, respectively. Noting this and further assuming that the neutral axis of the beam is inextensible result in a governing variational equation for the system, derived from extended Hamilton's principle, given by

$$\delta H = \delta\int_{t_1}^{t_2}\int_0^l \left\{\bar{L} + \frac{1}{2}\lambda[1-(1+u')^2-(v')^2]\right\} ds dt + \int_{t_1}^{t_2}\int_0^l (Q_u\delta u + Q_v\delta v) ds dt = 0 \tag{2}$$

where l represents the beam's undeformed length, λ denotes the

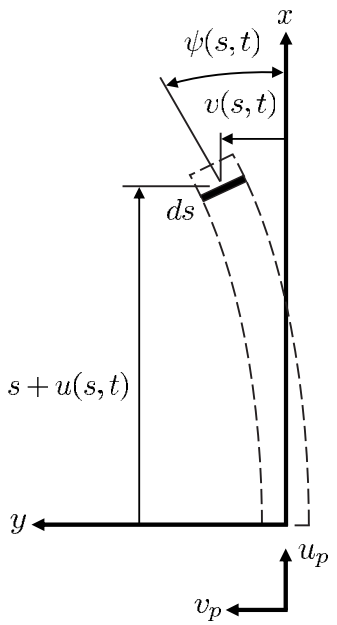

Fig. 1 Schematic of a representative mechanical parametric amplifier: a base-excited cantilevered beam

Lagrange multiplier used to maintain the inextensibility constraint,

$$(1+u')^2+(v')^2=1 \tag{3}$$

and Q_u and Q_v represent the generalized forces not accounted for in the specific Lagrangian, $\bar{L}$, in the u and v directions, respectively. Assuming that damping has an appreciable impact on only the local transverse motion of the beam, these forces can be approximated by

$$Q_u=-\rho Ag, \quad Q_v=-c\dot{v} \tag{4}$$

where g represents the beam's acceleration due to gravity and c represents a specific viscous damping coefficient. Substituting each of these forces, as well as the specific Lagrangian, into Eq. (2), integrating by parts successively, and introducing the kinematic constraint relating the angle ψ to the planar displacements u and v,

$$\tan\psi=\frac{v'}{1+u'} \tag{5}$$

results in a pair of coupled governing equations. The equation of motion governing transverse dynamics can be recovered from this set, by first solving the longitudinal equation to obtain the Lagrange multiplier and then substituting the obtained function into the second equation. Truncating the result such that only linear terms remain (only linear amplifier operation is deemed pertinent and practical here) yields a distributed-parameter system model given by

$$\rho A\ddot{v}+c\dot{v}+EIv^{iv}-v''\rho A\ddot{u}_p(s-l)-v'\rho A\ddot{u}_p-v''\rho Ag(s-l)-v'\rho Ag=-\rho A\ddot{v}_p \tag{6}$$

To reduce the number of free parameters in the system detailed above, it proves convenient to rescale Eq. (6). Accordingly, the arc length variable and beam displacements are scaled by the beam's undeformed length l and an additional characteristic length v_0 (e.g., the width or thickness of the beam), according to

$$\hat{s}=\frac{s}{l} \tag{7}$$

$$\hat{v}=\frac{v}{v_0}, \quad \hat{u}_p=\frac{u_p}{v_0}, \quad \hat{v}_p=\frac{v_p}{v_0} \tag{8}$$

and time is scaled by a characteristic period of the system, according to

$$\hat{t}=\frac{t}{T} \tag{9}$$

where

$$T=\sqrt{\frac{\rho Al^4}{EI}} \tag{10}$$

This renders a final distributed-parameter system model given by

$$\ddot{\hat{v}}+\hat{c}\dot{\hat{v}}+\hat{v}^{iv}-\frac{v_0}{l}\ddot{\hat{u}}_p(\hat{s}-1)\hat{v}''-\frac{v_0}{l}\ddot{\hat{u}}_p\hat{v}'-\frac{\rho Agl^3}{EI}(\hat{s}-1)\hat{v}''-\frac{\rho Agl^3}{EI}\hat{v}'=-\ddot{\hat{v}}_p \tag{11}$$

where

$$\hat{c}=\frac{cT}{\rho A} \tag{12}$$

Note that the derivative operators have been redefined here in terms of the new time and arc length variables, $\hat{t}$ and $\hat{s}$, respectively.

Though the beam's behavior could potentially be recovered from the distributed-parameter model presented in Eq. (11), a lumped-mass model proves sufficient for the present analysis. Accordingly, the dynamic variable $\hat{v}$ is decomposed into spatial and temporal components using the cantilever's first mode shape $\Phi(\hat{s})$, according to

$$\hat{v}=w(\hat{t})\Phi(\hat{s}) \tag{13}$$

The result is then projected back onto the first mode shape using an inner product operator yielding a final lumped-mass model given by

$$z''+2\varepsilon\zeta z'+z+[\varepsilon\lambda_1\Omega^2\cos(\Omega\tau+\phi)+\varepsilon\lambda_2\Omega^2\cos(2\Omega\tau)]z=\varepsilon\eta_1\Omega^2\cos(\Omega\tau+\phi)+\varepsilon\eta_2\Omega^2\cos(2\Omega\tau) \tag{14}$$

with nondimensional parameters and operators defined as in Table 1. Note that the imposed harmonic base motions included here are assumed to result from a unidirectional base excitation $\hat{x}_p$ given by

$$\hat{x}_p=\hat{A}\cos(\omega t+\phi)+\hat{B}\cos(2\omega t)=\hat{A}\cos(\hat{\omega}\hat{t}+\phi)+\hat{B}\cos(2\hat{\omega}\hat{t}) \tag{15}$$

and are defined according to

$$\hat{u}_p=\hat{x}_p\sin\alpha, \quad \hat{v}_p=\hat{x}_p\cos\alpha \tag{16}$$

Excitations of frequency ω are used to provide direct excitation to the system, while excitations of frequency 2ω are used for parametric pumping. Also note that the phase-dependent nature of this excitation is requisite in the examination of degenerate parametric amplification. An examination of nondegenerate amplification, which is phase independent and does not require the strict 2:1 frequency ratio utilized above, is left for subsequent studies.

3 Analysis

Though the equation of motion detailed in Eq. (14) is linear, its time-varying stiffness coefficient prevents the derivation of a *tractable* closed-form solution. Accordingly, the method of averaging is exploited here. To facilitate this approach, a constrained coordinate change is first introduced into Eq. (14), namely,

$$z(\tau)=X(\tau)\cos(\Omega\tau)+Y(\tau)\sin(\Omega\tau)$$

Table 1 Nondimensional parameter definitions. Note the ε represents a "small" parameter introduced for analytical purposes and ω represents the system's "physical" base excitation frequency.

$$z = w$$

$$\tau = \omega_0 \hat{t},\ (\bullet)' = \frac{d(\bullet)}{d\tau}$$

$$\hat{\omega} = \omega T,\ \Omega = \frac{\hat{\omega}}{\omega_0}$$

$$\omega_0^2 = \int_0^1 \Phi\Phi^{iv} d\hat{s} - \frac{\rho A l^3 g}{EI}\left(\int_0^1 \Phi\Phi''(\hat{s}-1)d\hat{s} + \int_0^1 \Phi\Phi' d\hat{s}\right)$$

$$\varepsilon\zeta = \frac{\hat{c}}{2\omega_0}$$

$$\varepsilon\lambda_1 = \frac{\hat{A} v_0 \sin\alpha}{l}\left(\int_0^1 \Phi\Phi''(\hat{s}-1)d\hat{s} + \int_0^1 \Phi\Phi' d\hat{s}\right)$$

$$\varepsilon\lambda_2 = \frac{4\hat{B} v_0 \sin\alpha}{l}\left(\int_0^1 \Phi\Phi''(\hat{s}-1)d\hat{s} + \int_0^1 \Phi\Phi' d\hat{s}\right)$$

$$\varepsilon\eta_1 = \hat{A}\cos\alpha \int_0^1 \Phi d\hat{s}$$

and

$$\varepsilon\eta_2 = 4\hat{B}\cos\alpha \int_0^1 \Phi d\hat{s}$$

$$z'(\tau) = -X(\tau)\Omega\sin(\Omega\tau) + Y(\tau)\Omega\cos(\Omega\tau) \tag{17}$$

Additionally, since near-resonant behavior is of particular interest, a detuning parameter σ defined by

$$\sigma = \frac{\Omega - 1}{\varepsilon} \tag{18}$$

is utilized. Separating the constraint equation, as well as that which results from substitution, in terms of X' and Y' and averaging the results over one period of the oscillator's response $(2\pi/\Omega)$ result in the system's averaged equations, which are given by

$$X' = -\tfrac{1}{4}\varepsilon(\lambda_2 Y + 4\sigma Y + 4\zeta X - 2\eta_1 \sin\phi) + \mathcal{O}(\varepsilon^2)$$

$$Y' = -\tfrac{1}{4}\varepsilon(\lambda_2 X - 4\sigma X + 4\zeta Y - 2\eta_1 \cos\phi) + \mathcal{O}(\varepsilon^2) \tag{19}$$

Using these averaged equations, the steady-state behavior of the system can be recovered by setting $(X', Y') = (0,0)$. This reveals that the system has a steady-state solution given, in terms of amplitude and phase, by

$$\bar{a} = 2\sqrt{\frac{\eta_1^2[\lambda_2^2 + 16(\zeta^2+\sigma^2) + 8\lambda_2(\sigma\cos 2\phi - \zeta\sin 2\phi)]}{[\lambda_2^2 - 16(\sigma^2+\zeta^2)]^2}} \tag{20}$$

$$\bar{\psi} = \arctan\left[\frac{(\lambda_2 - 4\sigma)\sin\phi - 4\zeta\cos\phi}{(\lambda_2 + 4\sigma)\cos\phi - 4\zeta\sin\phi}\right] \tag{21}$$

where

$$\bar{a} = \sqrt{\bar{X}^2 + \bar{Y}^2},\quad \bar{\psi} = \arctan\frac{\bar{Y}}{\bar{X}} \tag{22}$$

Utilizing this form of the oscillator's amplitude, the gain associated with the amplifier can be defined as

$$G = \frac{\bar{a}_{\text{pump on}}}{\bar{a}_{\text{pump off}}} = \frac{\bar{a}}{\bar{a}|_{\lambda_2=0}} \tag{23}$$

which at $\sigma = 0$ yields

$$G(\sigma = 0) = 4\zeta\sqrt{\frac{\lambda_2^2 + 16\zeta^2 - 8\lambda_2\zeta\sin 2\phi}{(\lambda_2^2 - 16\zeta^2)^2}} \tag{24}$$

Using Eqs. (20) and (24), the pertinent performance metrics of the mechanical amplifier can be readily identified.

Generally speaking, the resonator described herein can operate at any point within the λ_2-σ parameter space. However, due to the presence of parametric excitation in Eq. (14), the oscillator has a classical "wedge of instability" (Arnold tongue) structure associated with it (see Fig. 2) [16,17]. As such, parametric-resonance-induced oscillations, bounded by only by the system's mechanical nonlinearities, are possible for pump amplitudes greater than

$$\lambda_{2,\text{crit}} = 4\sqrt{\sigma^2 + \zeta^2} \tag{25}$$

As these motions are incompatible with linear signal amplification, the present study limits itself to operation below the

$$\lambda_2^2 - 16(\sigma^2 + \zeta^2) = 0 \tag{26}$$

threshold, which corresponds to the principal parametric resonance's wedge of instability. While the present work focuses on amplification near the system's principal instability zone (i.e., near $\sigma = 0$), it is important to note that amplification can be realized, at least in theory, by pumping the system near secondary instability regions as well. Given that these regions are quite difficult to identify and exploit experimentally, further discussion is omitted here.

With the limitation on pump amplitude (λ_2), detailed above, in place, the gain associated with the macroscale parametric amplifier can be readily characterized. Figure 3, for example, details the amplifier's gain as a function of pump amplitude. As expected, the gain monotonically increases with increasing pump amplitude, eventually approaching infinity as λ_2 approaches $\lambda_{2,\text{crit}}$ (as the system passes into parametric resonance). This is in direct contrast to the effect of increasing the amplitude of the amplifier's input signal (direct excitation), which has a negligible effect on the system's gain, as detailed in Eq. (24). Also evident from Fig. 3 is the potential for relatively high amplifier gains. As these gains require the ability to operate near, but not above, $\lambda_{2,\text{crit}}$, though, extremely large gains (i.e., multiple orders of magnitude) may be quite difficult to realize in the face of noise and system uncertainty.

To further reinforce the amplification seen in Fig. 3, frequency response curves for the mechanical amplifier operating under three distinct pump conditions are included in Fig. 4. Once again the effect of the parametric amplifier is evident, as gains of approximately 1.25 and 1.45 are realized with pump amplitudes well below $\lambda_{2,\text{crit}}$.

Though Figs. 3 and 4 detail the effect of the pump's amplitude on the amplifier's performance, as detailed in Eq. (24), the system gain also depends on the relative phase ϕ incorporated into the amplifier's input signal. Figure 5 details the effect of varying this phase in a representative amplifier. As evident, maximum gains are realized for a relative phase angle of $\phi = -45$ deg (and every 180 deg interval), where $\sin 2\phi$ is minimum. Likewise, minimum gains are realizable at $\phi = 45$ deg (and every 180 deg multiple), where $\sin 2\phi$ is maximum. The latter operating point reveals a

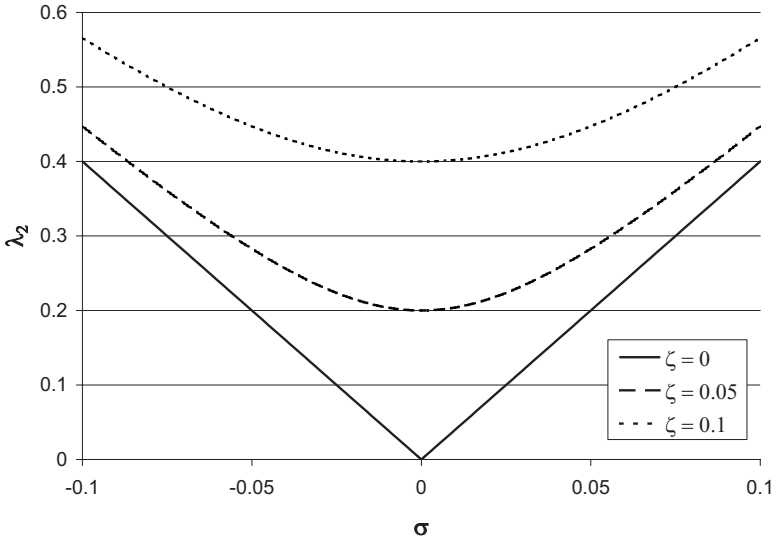

Fig. 2 Wedges of instability, recovered for various levels of damping, near $\sigma=0$. Note that successful linear parametric amplification requires that the system operates below its corresponding wedge, as parametric resonance occurs within the instability region.

potential application for parametric amplifiers which has received little attention and is targeted for future study: vibration suppression.

Before proceeding with an experimental investigation of the macroscale parametric amplifier, the noise characteristics of the device should be briefly noted. Given that the amplifier described herein is designed to operate in a degenerate phase-sensitive mode, it, in theory, should be noise free down to a quantum mechanical level [3,11,18]. In practice, minimal amounts of noise can be expected, but these noise contributions should be appreciably smaller than the 3 dB of noise typically attributed to phase-insensitive nondegenerate amplifiers [11].

4 Experimental Results

Though the preceding analytical investigation appears to verify the feasibility of a macroscale parametric amplifier, experimental results were deemed necessary to validate the analytical results detailed herein. Accordingly, the experimental setup depicted pictorially in Fig. 6 and schematically in Fig. 7 was assembled. The system's signal flow is outlined below.

To begin, a signal generator (Wavetek 2 MHz Variable Phase Synthesizer, model 650) is used to produce the two required input signals, one at the driving frequency ω and another at 2ω, with a fixed relative phase ϕ. These two signals are added together using

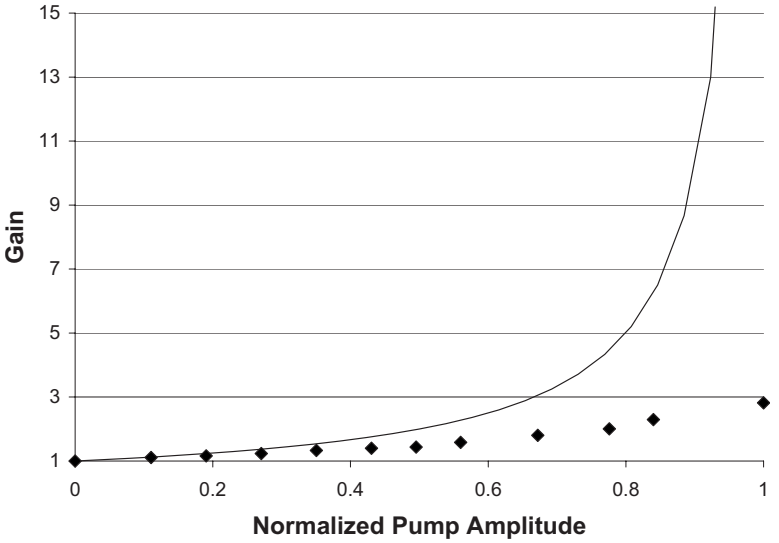

Fig. 3 Amplifier gain $G(\sigma=0)$ plotted versus normalized pump amplitude $\lambda_2/\lambda_{2,crit}$ for an oscillator operating at $\sigma=0$ with $\phi=-\pi/4$. Note that the pump amplitude has been normalized such that the parametric instability (be it analytically or experimentally determined) occurs at unity. Also note that in this figure lines are used to designate analytical results and data points are used to designate experimental results. Finally, note that here, and in Figs. 4 and 5, $\zeta=0.065$.

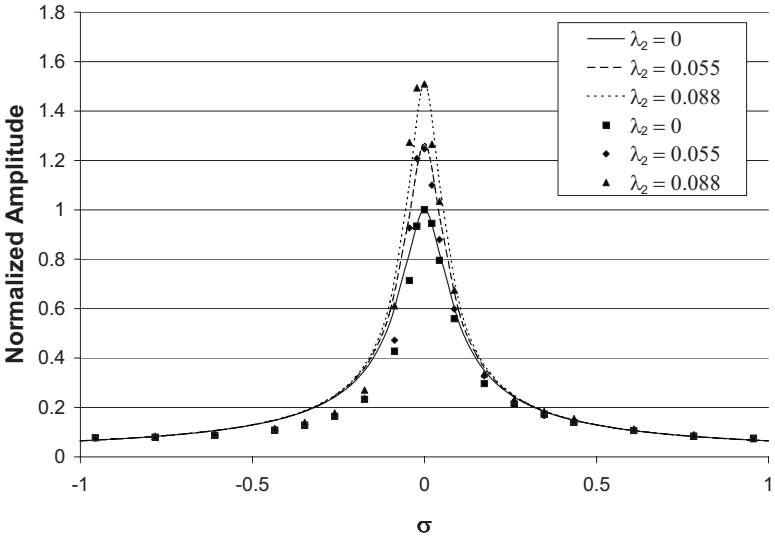

Fig. 4 Frequency response curves, $\bar{a}/\max\{\bar{a}(\lambda_2=0)\}$ versus σ, corresponding to three different values of λ_2 (pump amplitudes). Note that the responses have been normalized such that the unpumped system has a resonant amplitude of unity. Also note that in this figure, lines are used to designate analytical results and data points are used to designate experimental results.

a summing operational amplifier circuit, and the result is given as a command signal to the electromagnetic vibration exciter (MB Dynamics model PM-500). This exciter, in turn, provides base excitation to a cantilevered spring steel beam ($190\times19\times0.5$ mm^3, $f_1\approx11.5$ Hz, $f_2\approx73.3$ Hz), which is orientated at $\alpha=80$ deg to induce both direct and parametric excitations. To ensure that the shaker output matches that desired by the operator, the base excitation is measured using a three-axis accelerometer (Analog Devices ADXL105EM-3) attached directly to the exciter table. Beam deflections are measured using two strain gauges (Measurements Group Inc., Micro Measurements Division, EA-13-120LZ-120) mounted in a half-bridge configuration. The strain signal from these gauges is balanced and low-pass filtered (100 Hz cutoff frequency) by a signal conditioning amplifier (Measurements Group Inc., Instruments Division, Model 2210). For measurement purposes, the command, accelerometer, and strain signals are each recorded using an Agilent 54624A oscilloscope.

With the experimental test-rig depicted in Fig. 7 assembled, the beam's damping ratio ($\varepsilon\zeta\approx0.0065$) was determined using logarithmic decrement methods and the beam's response was recorded at discrete operating points over a wide range of forcing parameters (i.e., values of ϕ, $\hat{A}$, $\hat{B}$, etc.). Pertinent results recovered during experimentation are detailed below.

Figure 4, recovered by holding the vibration exciter's resonant direct excitation amplitude ($\hat{A}$) fixed and systematically varying both the excitation frequency (ω) and pump amplitude ($\hat{B}$), depicts the cantilevered beam's frequency response for three distinct

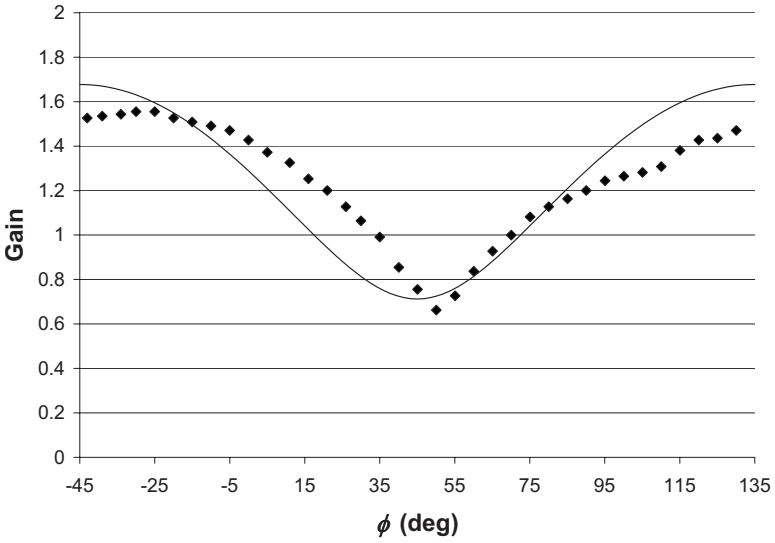

Fig. 5 Gain $G(\sigma=0)$ versus phase ϕ. Note that in this figure, lines are used to designate analytical results and data points are used to designate experimental results.

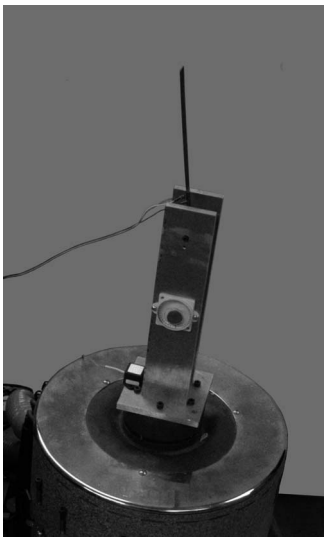

Fig. 6 The experimental setup used to obtain the results included in Figs. 3–5

pump values. As evident, the system exhibits a linear resonance at approximately 11.5 Hz, which varies in normalized amplitude from 1 to approximately 1.5 with varying pump amplitude. This is in close accordance with the predicted system behavior shown in Fig. 4, in terms of both Q and amplitude, and verifies that nonnegligible amplifier gains are experimentally realizable in a macroscale parametric amplifier. This conclusion is further reinforced by Fig. 8, which shows the system's resonant response when pumped and unpumped, and by Fig. 3, which depicts the amplifier's gain as a function of normalized pump amplitude. In the latter figure, as predicted analytically, the amplifier's gain is shown to increase with increasing pump amplitude ($\hat{B}$). However, while theory predicts multiple-order-of-magnitude gains, the experimentally acquired amplifier gains appear to only reach approximately 1.6 before the onset of parametric resonance (as verified by turning off the direct excitation signal, i.e., setting $\hat{A}=0$). Though this difference could be due to geometric or inertial nonlinearities, the symmetric nonhysteretic nature of the frequency response near this operating condition seems to indicate the presence of another limiting factor. Accordingly, the authors are currently exploring other reasons for this experimental gain limitation, including the effect that the nonresonant direct excitation has on the system's behavior near the onset of parametric resonance and the effect that noise and uncertainty have on the system's instability threshold.

To validate the phase-dependent nature of the degenerate amplifier, system behaviors akin to those illustrated in Fig. 5 were

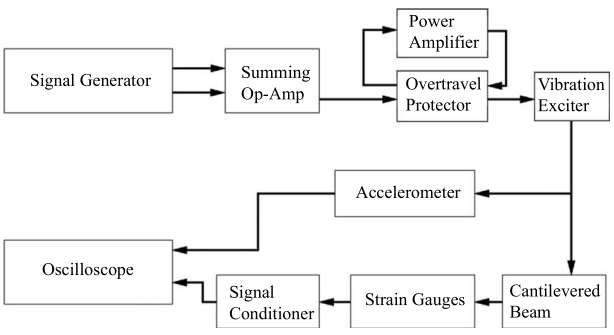

Fig. 7 Block diagram of the experimental setup used to obtain the results included in Figs. 3–5

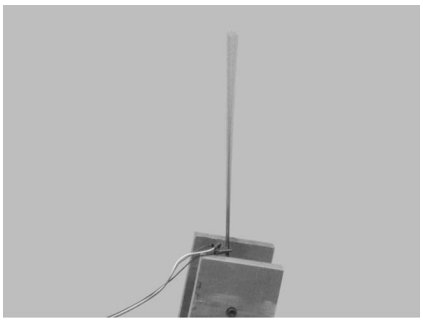

(*a*)

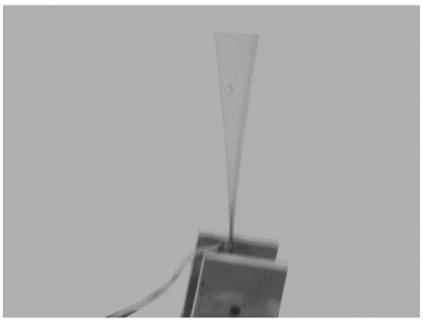

(*b*)

Fig. 8 The cantilever driven near resonance (*a*) without and (*b*) with a strong parametric pump

also examined experimentally. As evident, the system exhibits a phase-dependent amplitude, which varies between approximately 0.6 and 1.6 with varying ϕ. The maximum and minimum response amplitudes, as previously predicted, occur near −45 deg and 45 deg, respectively, and the phase relationship is repeated on 180 deg intervals. This is in close accordance with the present work's analytical findings.

5 Conclusion

As noted in the Introduction, parametric amplification has been implemented, to date, in a wide variety of electrical and micro- and nanomechanical systems. However, to the best of the authors' knowledge, few, if any, macroscale mechanical amplifiers have been reported. The present work fills this apparent void by demonstrating that parameter amplification can be easily realized in even the simplest of macroscale mechanical systems, including a base-excited cantilever with longitudinal and transverse excitations. Furthermore, the work demonstrates that nontrivial amplifier gains on the order of 1.4–1.6 are relatively easy to realize in practice and that appreciable gains may be recoverable with further study. Accordingly, mechanical amplifiers are believed to be of practical use in a wide variety of macroscale applications, including the amplification of output signals in some acoustic systems, such as cavity resonators, and vibration test equipment. Additionally, in certain applications, parametric amplification, with careful phase selection, may facilitate vibration suppression and thus offers a potential alternative to classical vibration absorbers, which typically require the implementation of additional hardware. Ongoing work is aimed at extending the results described herein to the aforementioned applications, as well as identifying the factor(s) limiting the mechanical amplifier's gain.

Acknowledgment

The authors would like to extend their gratitude to Dr. Alan Haddow and Mr. Umar Farooq for their assistance in preparing the experimental setup. It should also be noted that this material is

based on work supported by the National Science Foundation under Grant No. ECS-0428916.

References

[1] Mumford, W. W., 1960, "Some Notes on the History of Parametric Transducers," Proc. IRE, **48**(5), pp. 848–853.
[2] Louisell, W. H., 1960, *Coupled Mode and Parametric Electronics*, Wiley, New York.
[3] Rugar, D., and Grütter, P., 1991, "Mechanical Parametric Amplification and Thermomechanical Noise Squeezing," Phys. Rev. Lett., **67**(6), pp. 699–702.
[4] Carr, D. W., Evoy, S., Sekaric, L., Craighead, H. G., and Parpia, J. M., 2000, "Parametric Amplification in a Torsional Microresonator," Appl. Phys. Lett., **77**(10), pp. 1545–1547.
[5] Baskaran, R., and Turner, K. L., 2003, "Mechanical Domain Coupled Mode Parametric Resonance and Amplification in a Torsional Mode Micro Electro Mechanical Oscillator," J. Micromech. Microeng., **13**(5), pp. 701–707.
[6] Ouisse, T., Stark, M., Rodrigues-Martins, F., Bercu, B., Huant, S., and Chevrier, J., 2005, "Theory of Electric Force Microscopy in the Parametric Amplification Regime," Phys. Rev. B, **71**, 205404.
[7] Zalalutdinov, M., Olkhovets, A., Zehnder, A., Ilic, B., Czaplewski, D., Craighead, H. G., and Parpia, J. M., 2001, "Optically Pumped Parametric Amplification for Micromechanical Oscillators," Appl. Phys. Lett., **78**(20), pp. 3142–3144.
[8] Gallacher, B. J., Burdess, J. S., Harris, A. J., and Harish, K. M., 2005, "Active Damping Control in MEMS Using Parametric Pumping," *Proceedings of Nanotech 2005: The 2005 NSTI Nanotechnology Conference and Trade Show*, Anaheim, CA, May 8–12, Vol. 7, pp. 383–386.
[9] Raskin, J.-P., Brown, A. R., Khuri-Yakub, B. T., and Rebeiz, G. M., 2000, "A Novel Parametric-Effect MEMS Amplifier," J. Microelectromech. Syst., **9**(4), pp. 528–537.
[10] Olkhovets, A., Carr, D. W., Parpia, J. M., and Craighead, H. G., 2001, "Non-Degenerate Nanomechanical Parametric Amplifier," *Proceedings of MEMS 2001: The 14th IEEE International Conference on Micro Electro Mechanical Systems*, Interlaken, Switzerland, Jan. 21–25, pp. 298–300.
[11] Dana, A., Ho, F., and Yamamoto, Y., 1998, "Mechanical Parametric Amplification in Piezoresistive Gallium Arsenide Microcantilevers," Appl. Phys. Lett., **72**(10), pp. 1152–1154.
[12] Roukes, M. L., Ekinci, K. L., Yang, Y. T., Huang, X. M. H., Tang, H. X., Harrington, D. A., Casey, J., and Artlett, J. L., 2004, "An Apparatus and Method for Two-Dimensional Electron Gas Actuation and Transduction for Gas NEMS," International Patent WO/2004/041998 A2.
[13] Ono, T., Wakamatsu, H., and Esashi, M., 2005, "Parametrically Amplified Thermal Resonant Sensor With Pseudo-Cooling Effect," J. Micromech. Microeng., **15**(12), pp. 2282–2288.
[14] Crespo da Silva, M. R. M., and Glynn, C. C., 1978, "Nonlinear Flexural-Flexural-Torsional Dynamics of Inextensional Beams. I: Equations of Motion," J. Struct. Mech., **6**(4), pp. 437–448.
[15] Malatkar, P., 2003, "Nonlinear Vibrations of Cantilever Beams and Plates," Ph.D. thesis, Virginia Polytechnic Institute and State University, Blacksburg.
[16] Nayfeh, A. H., and Mook, D. T., 1979, *Nonlinear Oscillations*, Wiley-Interscience, New York.
[17] Stoker, J. J., 1950, *Nonlinear Vibrations in Mechanical and Electrical Systems*, Wiley, New York.
[18] Caves, C. M., 1982, "Quantum Limits on Noise in Linear Amplifiers," Phys. Rev. D, **26**(8), pp. 1817–1839.